Comparing satellite rainfall estimates with rain gauge data: Optimal strategies suggested by a spectral model

Thomas L. Bell
Laboratory for Atmospheres, NASA Goddard Space Flight Center, Greenbelt, Maryland, USA

Prasun K. Kundu
Goddard Earth Sciences and Technology Center, University of Maryland Baltimore County, Baltimore, Maryland, USA
NASA Goddard Space Flight Center, Greenbelt, Maryland, USA

Received 11 June 2002; revised 24 September 2002; accepted 2 October 2002; published 11 February 2003.

[1] The statistical problem of comparing rain gauge measurements to satellite rain-rate estimates over an area surrounding the gauge(s) is examined using a model of rainfall variability developed for studies of sampling error in averages of satellite data. The model is able to capture a number of important aspects of the space-time spectrum of rain-rate variability, including the interdependence of time and space scales of variability. Four parameters must be specified in the model. Sets of parameters have been obtained that fit the statistics of radar-derived rain rates over the eastern tropical Atlantic (from GATE) and the western tropical Pacific (from TOGA COARE). The model predicts that there is an optimal averaging time for gauge data when gauge averages are compared to average satellite rain-rates for a specified area around the gauge. The optimal averaging time ranges from minutes to days as the diameter of the area around the gauge is extended from 2 km to 200 km. The optimal averaging time shrinks as more gauges are added to the area viewed by the satellite, but the model suggests that even over fairly dense gauge networks it is necessary to compare averages of several hundred satellite overflights in order to bring the comparison error down to the 10% level. The possibility that comparisons of gauge data with satellite averages might be improved by weighting the gauge data differently depending on how close the gauge data are in time to the satellite overflights is investigated, and it is found that in some cases the variance of the comparison error can be reduced by a factor of two by using optimal time-dependent weighting. *INDEX TERMS:* 1833 Hydrology: Hydroclimatology; 1854 Hydrology: Precipitation (3354); 1869 Hydrology: Stochastic processes; *KEYWORDS:* validation, precipitation, remote sensing, stochastic, space-time

Citation: Bell, T. L., and P. K. Kundu, Comparing satellite rainfall estimates with rain gauge data: Optimal strategies suggested by a spectral model, *J. Geophys. Res.*, *108*(D3), 4121, doi:10.1029/2002JD002641, 2003.

1. Introduction

[2] Satellites are the only practicable means of monitoring rainfall on a global scale, but remote-sensing methods used to estimate rainfall from space-borne instruments are inexact. Quantitative use of the satellite products requires that they be accompanied by estimates of their accuracy, and along with the decades-long effort to improve satellite rain estimates there has been a parallel effort to compare the estimates from space with more direct observations taken from the ground in order to determine the error characteristics of the satellite estimates whenever possible. An especially extensive set of such studies of satellite algorithms is reviewed by *Ebert et al.* [1996].

[3] Since satellite-instrument estimates are inherently limited by the resolution of the instrument, loosely referred to here as the field of view (FOV), the satellite estimates represent rain rates averaged over areas similar in size to the instrument resolution [see, e.g., *Olson*, 1989], with additional blurring because the satellite estimate actually depends on the state of the column of atmosphere above the FOV-sized area rather than on the rain rate at the surface. Verifying such estimates with ground observations requires that accurate estimates of rain averaged over FOV-sized areas be provided. Hydrologists have been grappling with this type of problem since well before the needs for satellite verification arose, and it is a notoriously difficult one.

[4] There are many ground-based approaches to estimating area-averaged rain rate. Many involve remote-sensing methods such as radar. We will principally concern ourselves here with estimates made with rain gauges. Rain gauges have the advantage that they measure rain in a fairly direct manner, and the errors they make are generally easily understood and to a considerable extent quantifiable. Errors

0148-0227/03/2002JD002641$09.00

in measurements by well maintained gauges can include both random and systematic components, depending on the type of apparatus, the environment, and the rain itself. Wind effects are often the most important, and can lead to underestimates ranging from a few percent to ten or twenty percent, depending on rain rate, wind speed, and gauge type and exposure. For discussions of these issues, see, for example, *Nešpor and Sevruk* [1999], *Habib et al.* [1999], *Krajewski et al.* [2000], and *Serra et al.* [2001]. Gauges also have the advantage that they are relatively inexpensive to deploy and are located at many sites around the world. Aside from all the mishaps to which any mechanical or electrical apparatus left outdoors is prone, they have the major disadvantage that they measure only what is falling within an area a few tens of centimeters in diameter. Inferences about what might have fallen in the tens of square kilometers around the gauge can only be made to the extent that what the gauge encounters is representative of what happened in the surrounding area.

[5] Rain rates vary rapidly in time and space on the scale of human perceptions, as anyone who has watched rain falling over a large flat open area can attest, and the same can be said for both the larger scales accessible to radars and satellites and the smaller scales explored with acoustical and optical instruments. What a rain gauge measures can therefore represent what has occurred in its neighborhood only in an average sense at best. This question has been investigated by setting out arrays of rain gauges and comparing the rain totals obtained by each gauge. Gradients in the rain totals can sometimes persist and be explained by local topographic and meteorological influences. See, for just a few of many examples, *Court* [1960] and *Wood et al.* [2000]. The representativeness of each rain gauge must therefore be examined carefully for such influences.

[6] The problem of how well a gauge average agrees with the average rainfall in its vicinity has been extensively studied theoretically as well as empirically. Examples of such studies include *Rodríguez-Iturbe and Mejía* [1974a, 1974b], *Silverman et al.* [1981], and *Morrissey et al.* [1995]. A particularly interesting and extensive empirical study was carried out by *Rudolf et al.* [1994]. They showed that the rms difference of the gauge average from the true areal average appeared to depend in a simple way on the number of gauges in the area. A theoretical argument for a dependence similar to what they found is given by *McCollum and Krajewski* [1998], who also investigated the error levels in averages of rain gauge data used to estimate areal monthly averages as a function of spatial correlation of the rain gauge data. *Krajewski et al.* [2000] used rain gauge correlations found in U.S. data to make quantitative estimates of error levels for areal averages of such data.

[7] In comparing the average rain rate seen by gauges to the average of satellite estimates made in the vicinity of the gauges, a number of questions arise: (1) How much disagreement between the two averages is attributable to the fact that a gauge sees a very small area continuously, whereas the satellite sees a very large area around the gauge only intermittently? (2) What is the best time interval over which to compare the two averages? (3) Over what area around the gauge(s) should the satellite averages extend? (4) If the gauge data are available as a function of time (e.g., minute by minute, hour by hour), would it be better to use time-weighted averages of the gauge data with weightings determined by the overflight times of the satellite?

[8] The answers to these questions are not usually obvious. An important aspect of these problems is that the statistics of space and time averages of rain rate change with the amount of averaging. Daily rain gauge data are correlated over shorter distances than monthly rain data, as can be inferred, for example, from the correlation lengths of order 10^1–10^2 km seen for daily rainfall by *Abtew et al.* [1995] and *Ciach et al.* [1997], as opposed to the correlation lengths of many hundreds of kms seen for monthly rainfall by *Mooley and Ismail* [1982] and *Morrissey* [1991]. Small-area averages of radar-derived rain rates are correlated over shorter times than large-area averages, as was shown, for example, by *Laughlin* [1981]. Determining the answers directly from data without the aid of a statistical model can be frustrating because of the inherent noisiness of rain statistics, so that extremely long averaging times are required in order to get stable results.

[9] A number of theoretical studies of the problem of comparing averages of satellite rain estimates with averages of data from one or more gauges have been carried out. The studies by *North and Nakamoto* [1989], *Graves et al.* [1993], *North et al.* [1994], and *Yoo et al.* [1996], in particular, used stochastic models in which time and space scales are interrelated. The studies emphasize the use of Fourier-transform methods, but the mathematical framework used in these studies is otherwise similar to what is used here.

[10] In earlier studies, error levels in satellite/gauge comparisons were estimated for specified averaging areas and time intervals. In this paper we shall explore how satellite/gauge comparisons change with averaging areas and times. The questions posed above will be examined with the aid of a model of rainfall statistics that was primarily developed for studies of sampling errors in monthly averaged satellite estimates of rainfall [*Bell and Kundu*, 1996] (hereinafter BK96). It is able to describe the changes in rainfall statistics with averaging times and averaging areas mentioned above to an impressive degree, and is therefore in that respect well suited to the study of these problems. Only second-order moment statistics of rain (variances, correlations) are described by the model, however, and the model cannot address problems having to do with the higher-moment statistics of rain without additional assumptions. See *Ha and North* [1999] and *Ha et al.* [2002] for examples of satellite/gauge comparisons that make use of information about whether or not rain is detected by the gauges and therefore involve statistics of the rain beyond space-time covariances.

[11] Section 2 describes a framework for investigating how much satellite and gauge averages tend to differ due to their different observational characteristics. Section 3 describes the statistical model used in the study and its ability to handle different time and space scales. Section 4 explores a number of different averaging schemes and shows that there is often an optimal scale for comparison. Section 5 raises the possibility of using time-varying weighted averages of gauge data to help reduce sampling error in satellite/gauge comparisons. The results are dis-

cussed in section 6. Mathematical details of some of the calculations are given in two appendices.

2. Comparing Satellite and Gauge Averages

[12] Comparisons of single, ''instantaneous,'' coincident observations by satellites and rain gauges tend not to be very informative since, as we shall see, their very different sampling characteristics introduce too much uncertainty into the comparison. In addition, the instantaneous satellite estimates for single FOVs are themselves commonly believed to have errors of order 50% or more [see, e.g., *Wilheit*, 1988; *Olson et al.*, 1996]. Errors in satellite estimates for the average rain rate in a FOV will be referred to here as retrieval errors. The many sources of these errors are reviewed by *Berg and Avery* [1995]. The goal in comparing averages of satellite rain-rate estimates to averages of rain gauge data is finding evidence (or lack of it) for bias in the satellite estimates.

[13] Biases in satellite estimates cannot be represented by a single number. They almost certainly vary with the kinds of rain being observed, the amounts, and a host of meteorological and climatological factors that will take long and patient research to unravel. The most informative comparisons of satellite and gauge averages will therefore be ones where just enough averaging is done to reduce the variability in the differences due to random sampling and retrieval error to a level where residual bias is detectable at a certain desired level. Large data sets consisting of long sequences of satellite observations in the neighborhood of rain gauges and the accompanying gauge data will need to be broken down into comparisons of subsets of observations, and indications of apparent bias examined for patterns that might indicate problems with the satellite retrievals in certain situations. For example, if the bias seemed to vary with the amount of stratiform precipitation, such a dependence might be revealed by comparing the biases seen in low-stratiform-amount and high-stratiform-amount cases. For this to be an effective approach the averaging must be sufficient to bring out the bias, but not so great that it reduces the data set to too few cases.

[14] As mentioned above, we expect averages of satellite data and of rain gauge data to differ because they each include rain observations that the other does not. This difference is referred to here as the error due to sample differences, or sampling error. There are also a number of other reasons the two averages might differ: the rain may not fall with equal probabilities at different times of the day, for example, or the mean rainfall may differ at different points (e.g., in hilly areas or near coasts). To the extent possible, the averages of the data must be adjusted to reduce the error due to these inhomogeneities to an acceptable level. The studies described here were originally motivated by questions about using gauge data from isolated, small atolls or oceanic buoys (as described by *McPhaden et al.* [1998], for example), where spatial and temporal inhomogeneities in the statistics tend to be less problematic. Environmentally complex areas may require either that the gauge density be high or that satellite/gauge comparisons be carried out at a more qualitative level.

[15] Let us first consider a simple example of the kinds of satellite/gauge comparisons one might wish to investigate, the difference between the average of satellite FOV estimates made in the neighborhood of a gauge during a single overflight of the gauge by the satellite and the average rain rate recorded by the gauge in a time interval bracketing the overflight time. Assume that the satellite overflight time occurs at $t = 0$ and that the rain gauge is located at position $\mathbf{x} = 0$, with $\mathbf{x} = \{x, y\}$. The average rain rate seen by the gauge over a time interval T is

$$R_{\mathrm{g}} = R_T(\mathbf{x} = 0) \tag{1}$$

with

$$R_T(\mathbf{x}) \equiv \frac{1}{T}\int_{-T/2}^{T/2} dt\, R(\mathbf{x}, t), \tag{2}$$

where $R(\mathbf{x}, t)$ is the rain rate at point $\mathbf{x}$ at time t, and the rain rate over the gauge orifice has been approximated by the rain rate at the point $\mathbf{x} = 0$.

[16] The satellite, on the other hand, is treated as providing an estimate of the average rain rate over an area A at time $t = 0$,

$$R_{\mathrm{s}} = R_A(t = 0) \tag{3}$$

with

$$R_A(t) \equiv \frac{1}{A}\int_A d^2\mathbf{x}\, R(\mathbf{x}, t), \tag{4}$$

where A is a circle of radius a with area $A = \pi a^2$. See the illustration in Figure 1. It would of course be possible to include several gauges and/or many satellite overflight times in the above averages, or to average over a rectangular area instead of a circular area. We will return to these questions later.

[17] The satellite can only provide an estimate of R_{s} in (3) as an average of the FOV estimates that fall within the circular area A. When the area A is comparable in size to an FOV, the precise location of the gauge within the FOV matters. As we shall see later, however, our analysis suggests that averages over relatively large areas around the gauge are preferable, and, anticipating that, we will ignore the complication of specifying where the gauge is on the scale of satellite FOVs.

[18] A bias in the satellite estimates is identified when the difference

$$\Delta R = R_{\mathrm{s}} - R_{\mathrm{g}} \tag{5}$$

is larger than can be accounted for by the sampling differences of the two systems or by random retrieval and measurement errors. If there is no bias in the estimates, ΔR should, on average, be zero. In order to test for the presence of a bias, we require an estimate of the random error components in ΔR. The mean squared difference of the averages is a useful measure of the error levels in the difference, defined as

$$\begin{aligned}\sigma^2 &\equiv \left\langle \left(\hat{R}'_{\mathrm{s}} - \hat{R}'_{\mathrm{g}}\right)^2 \right\rangle \\ &\approx \sigma^2_{\mathrm{samp}} + \sigma^2_{\mathrm{err,s}} + \sigma^2_{\mathrm{err,g}},\end{aligned} \tag{6}$$

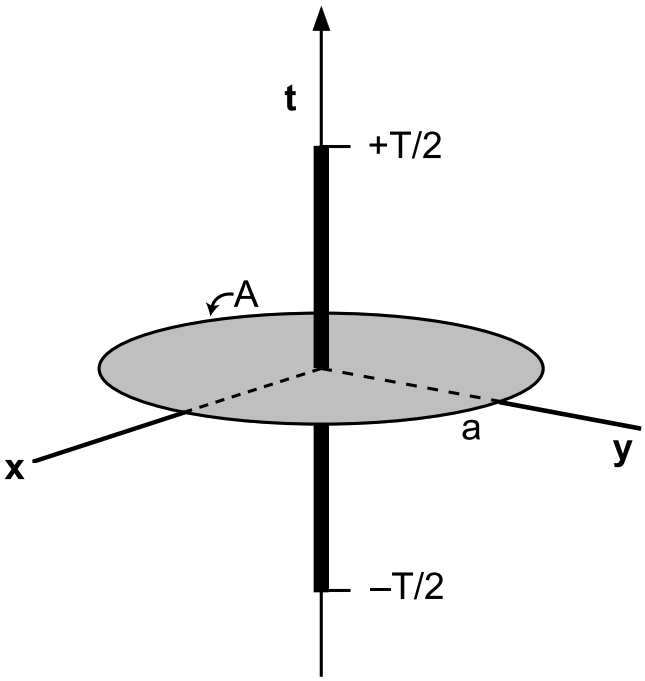

Figure 1. Comparison of average rain rate over a period T observed by a gauge located at the center of an area A of radius a, when the area A is observed at $t = 0$ by a satellite.

where $\hat{R}_s$ and $\hat{R}_g$ are the satellite and gauge estimates of R_s and R_g in (3) and (1), respectively, with (unknown) estimation errors included and where the error variances in (6) are defined as

$$\sigma^2_{\text{samp}} = \left\langle \left(R'_s - R'_g\right)^2 \right\rangle, \tag{7}$$

$$\sigma^2_{\text{err,s}} = \left\langle \left(\hat{R}'_s - R'_s\right)^2 \right\rangle, \tag{8}$$

$$\sigma^2_{\text{err,g}} = \left\langle \left(\hat{R}'_g - R'_g\right)^2 \right\rangle. \tag{9}$$

Angular brackets indicate an average over an ensemble of meteorological situations similar to the one for which we are trying to estimate σ^2, and primes indicate deviations from the ensemble mean; i.e., $z' \equiv z - \langle z \rangle$.

[19] In writing equation (6) it is implicitly assumed that sampling errors due to nonoverlapping coverage, satellite retrieval errors, and gauge measurement errors are uncorrelated with each other. It is difficult to think of a plausible physical mechanism that would produce such correlations, particularly correlations of sampling error with either retrieval or gauge errors. Correlations between retrieval and gauge errors might be generated if satellite retrievals had a rain-type-dependent bias (e.g., a tendency to overestimate stratiform rain amounts and to underestimate convective rain amounts), and the gauges used in the comparisons had a rain-type-dependent bias (e.g., due to changes in surface winds with rain type). In such a situation retrieval and gauge errors would vary in concert with rain type. For lack of quantitative estimates of the true sizes of the cross-correlation terms omitted from the right-hand side of (6), their contributions, if any, are neglected in estimating σ^2.

[20] A typical comparison of satellite estimates with gauge averages results in a scatter plot of the satellite averages versus the gauge averages for the same areas and time periods. The quantity σ in equation (6) is a measure of the amount of scatter about the "ideal" 45° line on which the points would lie if the satellite estimates were perfect and the gauge averages gave the true rain rate over the area sampled by the satellite. (Proper account of the "error-in-variable" problem must be taken in comparing the satellite and gauge data [see, e.g., *Fuller*, 1987].). In this paper we will concentrate on estimating the sampling error term in (6) based on models of the statistics of the "true" surface rain rates being estimated by the satellite and the gauge. Because a considerable amount of averaging (large A and T) is needed to reduce the error variance σ^2 to acceptable levels, the contributions to σ^2 by random retrieval and measurement errors represented by $\sigma^2_{\text{err,s}}$ and $\sigma^2_{\text{err,g}}$ tend to be considerably reduced, so that σ^2 is dominated by σ^2_{samp}, but this needs to be checked for each validation study.

[21] If a good estimate of σ can be obtained, one can conclude that if $|\Delta R| > 2\sigma$, there is a strong probability (>95%) that a bias exists—always assuming that inhomogeneities in the rain statistics have been compensated for and that the gauge data are accurate. The estimated bias in the satellite estimate would be

$$\text{Satellite bias} = \Delta R \pm \sigma, \tag{10}$$

with "one-sigma" confidence limits. In the analyses that follow, determination of bias at the 10% level is used as a reasonable goal, i.e., $\sigma_{\text{samp}} < 0.1\ R$, where R is the mean rain rate in the locality.

[22] The sampling error variance defined in (7) can be written in terms of the covariance of rain rate at two points separated in space by $\mathbf{r}$ and in time by τ,

$$c(\mathbf{r}, \tau) = \langle R'(\mathbf{x} + \mathbf{r}, t + \tau) R'(\mathbf{x}, t) \rangle, \tag{11}$$

which is assumed to depend only on the separation of the points $\{\mathbf{r}, \tau\}$. If (1) and (3) are substituted into the definition for σ^2_{samp} in (7), we can use (11) to write (7) as

$$\sigma^2_{\text{samp}} = c_{ss} + c_{gg} - 2c_{sg} \tag{12}$$

with

$$c_{ss} \equiv \left\langle \left(R'_s\right)^2 \right\rangle = \frac{1}{A^2} \int_A d^2\mathbf{x}_1 \int_A d^2\mathbf{x}_2 c(\mathbf{x}_1 - \mathbf{x}_2, 0), \tag{13}$$

$$c_{gg} \equiv \left\langle \left(R'_g\right)^2 \right\rangle = \frac{1}{T^2} \int_{-T/2}^{T/2} dt_1 \int_{-T/2}^{T/2} dt_2 c(0, t_1 - t_2), \tag{14}$$

and

$$c_{sg} \equiv \left\langle R'_s R'_g \right\rangle = \frac{1}{AT} \int_{-T/2}^{T/2} dt \int_A d^2\mathbf{x}\, c(\mathbf{x}, t). \quad (15)$$

[23] In the next section we describe a model for the rain-rate covariance (11) that was developed to estimate the sampling error in monthly averages of satellite data for a given area relative to the true monthly average that would have been obtained if the satellite were capable of continuous observation of the area. The model parameters were adjusted to fit the statistics of radar data over oceanic sites during two field campaigns, the Global Atmospheric Research Program (GARP) Atlantic Tropical Experiment (GATE) [*Houze and Betts*, 1981] and the Tropical Ocean Global Atmosphere (TOGA) Coupled Ocean-Atmosphere Response Experiment (COARE) [*Webster and Lukas*, 1992]. Given such a model, calculations of sampling error of satellite/gauge comparisons like the one described above can be carried out. These will be discussed in the following sections.

3. Spectral Model of Rain-Rate Covariance

[24] The model is described in BK96. Its four parameters characterize the space-time covariance of rain rate (11) needed for calculations like the one described in the previous section. It captures an aspect of rain behavior that is not always represented in statistical models of rain: timescales of variations in area-averaged rain rate become longer as the area is increased, and spatial correlations of time-averaged rain become longer as the time interval is lengthened. This phenomenon is partially captured by statistical models describing rain as randomly created cells, within which daughter cells are grown randomly, which in turn themselves grow daughter cells, etc., with faster and faster timescales and smaller and smaller spatial scales [e.g., *Waymire et al.*, 1984; *Rodríguez-Iturbe et al.*, 1987; *Smith and Krajewski*, 1987]. The present model was originally motivated by a model developed by *Bell* [1987] that used spectral methods to establish the space-time statistics of the rain being modeled. It is in some respects a generalization of the diffusive model of *North and Nakamoto* [1989].

[25] Although the model is described in detail in BK96, we review it briefly here in order to introduce the parameters needed for the computations. The space-time covariance of point rain rates (11) is expressed in terms of the Fourier transform in space and time of a spectral power function,

$$c(\mathbf{x}, \tau) = (2\pi)^{-3/2} \int_{-\infty}^{\infty} d\omega \int_{-\infty}^{\infty} dk_x \cdot \int_{-\infty}^{\infty} dk_y\, e^{i(\mathbf{k}\cdot\mathbf{x} - \omega\tau)} \tilde{c}(\mathbf{k}, \omega), \quad (16)$$

where $\mathbf{k}$ is a 2-dimensional wavevector $\{k_x, k_y\}$. The spectral power is given in this model by

$$\tilde{c}(\mathbf{k}, \omega) = \frac{F_0}{\omega^2 + 1/\tau_k^2}, \quad (17)$$

$$\tau_k = \frac{\tau_0}{\left(1 + k^2 L_0^2\right)^{1+\nu}}, \quad (18)$$

with $k = |\mathbf{k}|$. There are 4 parameters in the model, F_0, ν, L_0, and τ_0. The timescale for fluctuations with spatial wavelength $2\pi/k$ is τ_k. It gets longer as the wavelength gets larger, approaching τ_0 for wavelengths longer than L_0. Area-averaged instantaneous rain rate, when the area is large (for example, the area seen in one 360° scan by a radar), has a correlation time τ_0 in the model. Time averages of point rain rates, when the averaging time is long (as, for example, monthly averaged rain gauge data), have a correlation length L_0. Spatial variability at small scales increases as the exponent ν becomes more negative. Values of ν must lie within the range $-1/2 < \nu \leq 0$. All variances and covariances in the model are proportional to F_0. See BK96 for details about the motivation and interpretation of the model.

[26] The model will be specified in terms of the 4 parameters γ_0, ν, L_0, and τ_0, with γ_0 defined for convenience by

$$F_0 = \sqrt{2/\pi}\,\Gamma(1+\nu)\left(L_0^2/\tau_0\right)\gamma_0, \quad (19)$$

where $\Gamma(n)$ is the Euler gamma function. Model parameters were obtained in BK96 that best fit the statistics of radar-derived rain-rate maps over the eastern Atlantic produced in GATE [*Hudlow and Patterson*, 1979].

[27] P. K. Kundu and T. L. Bell (A stochastic model of space-time variability of tropical rainfall, 1, Statistics of spatial averages, submitted to *Water Resources Research*, 2002) recently obtained model fits to radar-derived rain data collected over an area in the western tropical Pacific during TOGA COARE. Radar observations were used from two ships designated "MIT" and "TOGA" during three cruises, each providing about four weeks of data [*Short et al.*, 1997]. Data used from the cruises spanned the periods

$$\begin{aligned} &\text{Cruise 1 : 11 Nov. to 10 Dec. 1992,} \\ &\text{Cruise 2 : 15 Dec. 1992 to 18 Jan. 1993,} \\ &\text{Cruise 3 : 23 Jan. to 23 Feb. 1993.} \end{aligned} \quad (20)$$

Separate sets of parameters were obtained for each ship for each cruise. The parameter values for which the model best fits the data statistics are given in Table 1, as well as the mean rain rate R for each case. (The mean rain rate may be thought of as a "5th" parameter of the model, although it is not used in specifying the model spectrum.) Length and time scales for GATE, as represented by the model parameters L_0 and τ_0, tend to be larger than the corresponding TOGA COARE parameters, which may reflect greater contributions to GATE rainfall by large-scale systems during the observation period. The variability among the TOGA COARE parameter values ν, L_0 and τ_0 is probably representative of the uncertainties in the parameter values because of the lengths of the observation periods (i.e., "sampling error"). Substantially more rain fell during Cruise 2 than the other two cruises, and this is reflected in the larger values of the parameters γ_0 and R.

[28] Since the model parameters in Table 1 were obtained from gridded radar data with grid spacings of 4 km for

Table 1. Parameter Values for Rain-Rate Covariance Model[a]

Data Set	γ_0, mm^2 h^{-2}	ν	L_0, km	τ_0, h	R, mm h^{-1}	σ_A^2, mm^2 h^{-2}
GATE Phase I	1.0	−0.11	104.	13.0	0.50	0.461
TOGA Cruise 1	0.067	−0.335	94.06	6.8	0.139	0.039
MIT Cruise 1	0.086	−0.297	73.89	5.8	0.134	0.032
TOGA Cruise 2	0.616	−0.239	53.81	5.0	0.351	0.127
MIT Cruise 2	0.206	−0.205	70.40	8.2	0.229	0.062
TOGA Cruise 3	0.127	−0.290	61.04	5.2	0.155	0.035
MIT Cruise 3	0.180	−0.259	64.94	4.5	0.200	0.052

[a]Parameters for the model spectrum, defined in (16), (17), and (18), from fits to radar data from Phase I of GATE and from the ships MIT and TOGA during the three TOGA COARE cruises listed in (20). Average rain rate for each data set and model-predicted variance of instantaneous area-averaged rain rate for a 314-km-diameter circle with the same area as a 2.5° × 2.5° square are given in the last two columns.

GATE and 2 km for TOGA COARE and covering a time period of 2–4 weeks, it is not obvious that the model can successfully describe the smaller scale statistics of rain gauge data nor the statistics of long time averages of gauge data, although it does quite well at fitting the data over the range of scales available in the radar data. To investigate the model's behavior on different scales, its predictions for the spatial correlation of time-averaged gauge data can be obtained by using an equation like (14) with "0" replaced by the separation of the two gauges. A formula for the spatial correlations is given in Appendix A in equation (A23).

[29] Figure 2 shows the spatial correlations for 15-min-averaged gauge data predicted by the model using parameter values in Table 1. As can be seen from Figure 2, the model with TOGA COARE parameters predicts correlation lengths ranging from about 8 km to 16 km (as measured by where the correlation falls to $1/e$), whereas the GATE parameters predict a correlation length of about 35 km. There were unfortunately not enough gauges deployed during TOGA COARE and GATE to test these predictions against actual gauge data. The TOGA COARE correlation lengths are comparable to what were found for a gauge array near Melbourne, Florida, by *Habib et al.* [2001], who found correlation lengths of about 4–5 km for 15-min-averaged gauge data for August–September 1998.

[30] On the other hand, correlations of monthly averaged gauge data (Figure 3) are predicted by the model to have spatial correlation lengths of about 50–80 km for TOGA COARE and about 145 km for GATE. Again, gauge statistics for these cases are unavailable, but *Krajewski et al.* [2000] found correlation lengths of order 200–460 km for summertime monthly averages from 14 U.S. gauge arrays, and *Morrissey* [1991] found correlation lengths of order 500 km for Pacific atoll rain gauges, perhaps a factor of 2 to 3 larger than what the model with the parameter values in Table 1 predicts. This suggests that the effects of large-scale variations in rainfall occurring over periods of a month or more are, not surprisingly, underestimated in the statistics for 3–4 weeks of radar data such as were used in obtaining the parameters in Table 1. Predictions using the model with the parameters in Table 1 must therefore be

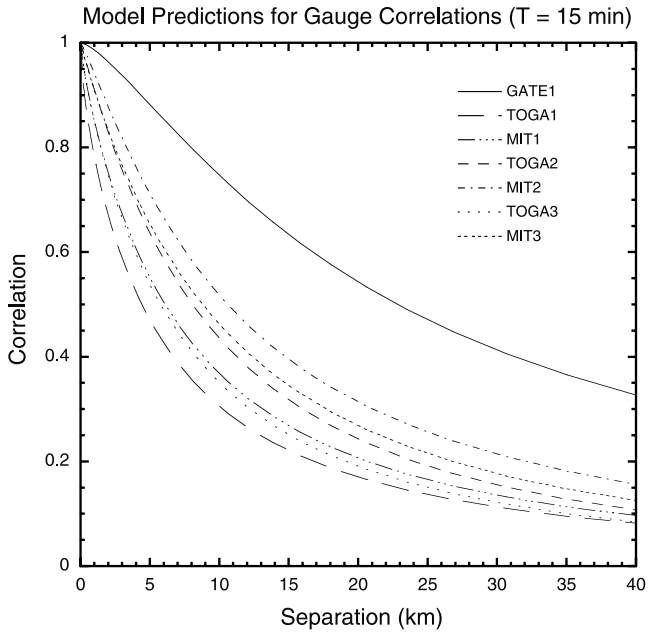

Figure 2. Predictions of spatial correlations of 15-min-averaged gauge data by spectral model using parameter values in Table 1. Correlations $c_{TT}(b)/c_{TT}(0)$ are plotted versus separation b using equation (A23) in Appendix A.

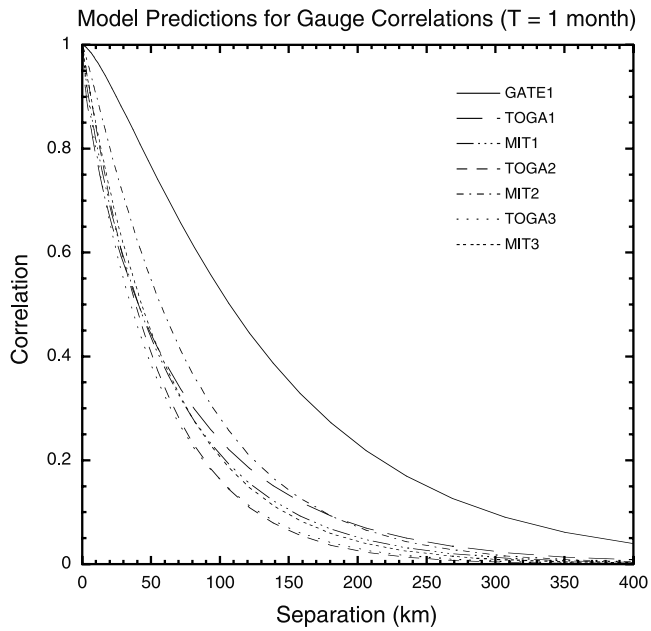

Figure 3. Predictions of spatial correlations of monthly averaged gauge data. Note change of scale of abscissa from Figure 2.

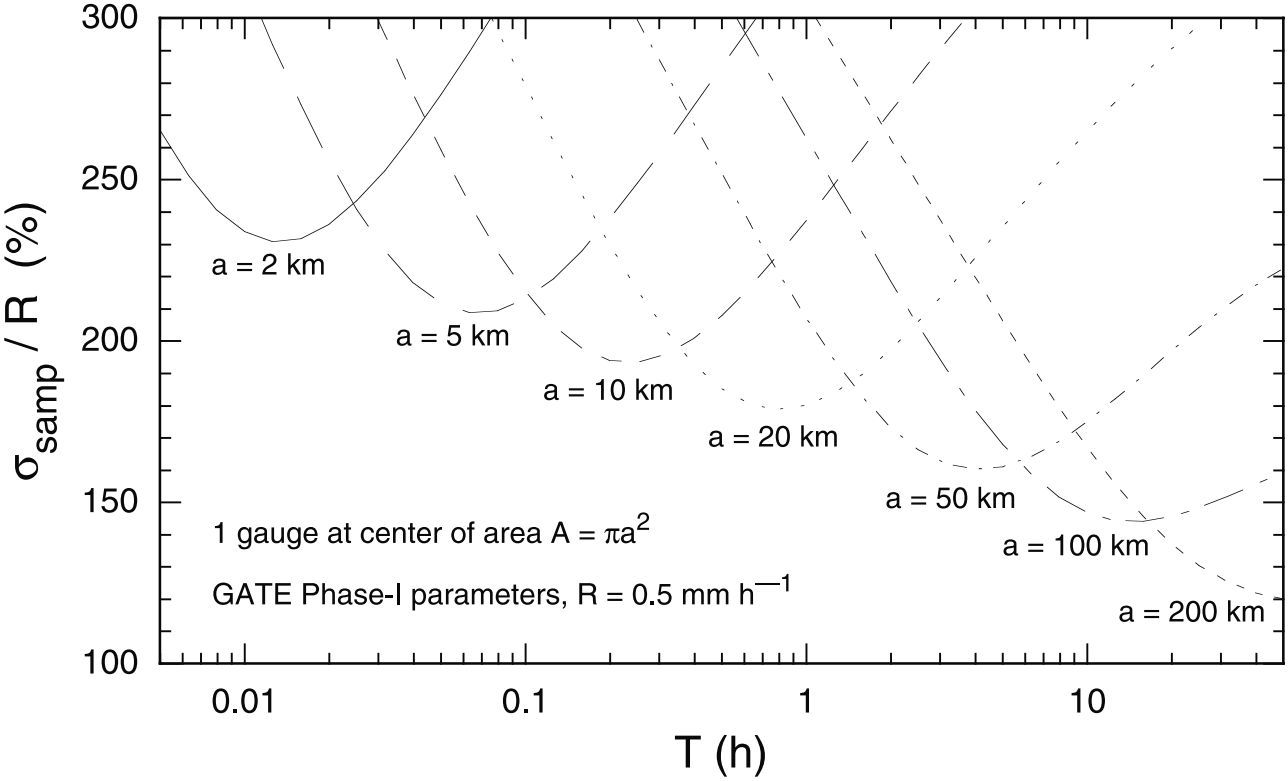

Figure 4. Model predictions of relative sampling error for comparisons of a single satellite overflight over an area A of radius a to a gauge average over an interval T bracketing the overflight time, as depicted in Figure 1.

tempered by these considerations. We will return to this issue in the discussion at the end.

4. Sampling Errors for Validation

[31] In this section we will explore the behavior of sampling error in the differences between satellite observations over an area surrounding one or more gauges for various averaging times T and averaging areas A. All of the calculations are done using circular areas rather than using square, grid box shaped areas. The difference in the results should be very small if the areas are equal in magnitude. For example, the last column of Table 1 shows the variance of instantaneous area-averaged rain rate calculated from the model for each set of parameters listed in the table for a 314-km-diameter circle, using (A9). At the equator, a 2.5° × 2.5° square box has the same area as the circle. When variances of area-averaged rain rate are calculated for the square area using the spectral model, they are found to be smaller than the values for the circle by only about 1.5%.

4.1. Single Satellite Overflight, Single Gauge

[32] As a first example, consider the problem of comparing an average of satellite estimates from a single overflight of an area A with an average rain rate seen by a gauge over an interval of time T bracketing the overflight time of the satellite, as sketched in Figure 1. The rms difference σ_{samp} between the two averages can be calculated using (12) and the model covariance (16)–(18). Results for σ_{samp}/R are plotted in Figure 4 using the GATE model parameters from Table 1. A number of conclusions are illustrated by this figure: (1) Comparisons of a single-gauge average with one satellite pass are, not surprisingly, extremely noisy, as evidenced by relative errors considerably larger than 100%, no matter what the averaging time T. (2) The comparisons become less noisy as the area averaged over increases. (3) Less obviously, for a given area A there is an optimal accumulation interval T for the gauge, and T increases as the satellite averaging area A increases.

[33] These sampling error results depend on the rain statistics. Model predictions (not shown) for σ_{samp}/R are considerably higher when the TOGA COARE parameter values in Table 1 are used, especially for the smaller areas A. This is largely due to the fact that the TOGA COARE statistics suggest higher spatial variability at small scales than for GATE, as evidenced by the larger negative values of the exponent ν in Table 1.

4.2. Single Satellite Overflight, Gauge Array

[34] As a second example, consider the problem of comparing a satellite average over an area A where an array of gauges is present, thus providing a better estimate of the area-averaged rain rate in A than a single gauge can. In such a case, the gauge average in equation (1) is replaced by the n-gauge average

$$R_{n\text{g}} = \frac{1}{n}\sum_{i=1}^{n} R_T(\mathbf{x}_i), \tag{21}$$

where the locations of the n gauges are specified by the positions $\mathbf{x}_i$, $i = 1, \ldots, n$. We must then calculate an

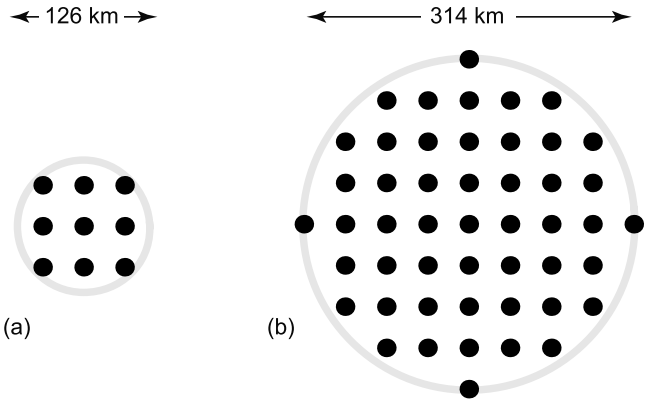

Figure 5. Idealized distribution of gauges with a density similar to that of the Oklahoma Mesonet. Inter-gauge distance is 39 km. (a) Circular area with a = 63 km with same area as a 1° × 1° grid box (9 gauges); and (b) circular area with a = 157 km with same area as a 2.5° × 2.5° grid box (49 gauges).

expression like (7) with R_g replaced by R_{ng}. The term c_{gg} is replaced by the double-sum expression

$$c_{ng,ng} = \frac{1}{n^2}\sum_{i=1}^{n}\sum_{j=1}^{n}\langle R'_T(\mathbf{x}_i)R'_T(\mathbf{x}_j)\rangle, \tag{22}$$

which can be calculated from the spectral model using the covariance $c_{TT}(|\mathbf{x}_i - \mathbf{x}_j|)$, an expression for which is obtained in Appendix A (equation A23). Likewise, the cross-term c_{sg} in (7) is replaced by the n-gauge expression

$$c_{s,ng} = \frac{1}{n}\sum_{i=1}^{n}\langle R'_A R'_T(\mathbf{x}_i)\rangle, \tag{23}$$

which can be calculated from the model using the covariance $c_{AT}(|\mathbf{x}_i|)$ given by (A20) in Appendix A.

[35] As an example of such a situation, consider the sort of comparisons that might be possible over the Oklahoma Mesonet described by *Brock et al.* [1995]. About 100 gauges are distributed over an approximate 3° × 5° area, with an average inter-gauge distance of about 40 km. Suppose satellite estimates over grid box areas of order 1° × 1° or 2.5° × 2.5° are compared to averages of data from gauges within these areas. In order to make the model calculations easier, we consider an idealized version of this problem in which gauges are equally spaced within circular disks with the same area as the grid boxes, i.e., with radii a = 63 km and a = 157 km respectively. Figure 5 shows a sketch of the areas with the assumed gauge positions marked. Based on this configuration, the sampling error for comparison of a single overflight of the array by a satellite can be computed using the n-gauge analogue to equation (12),

$$\sigma^2_{ng,\mathrm{samp}} = c_{ss} + c_{ng,ng} - 2c_{s,ng} \tag{24}$$

using expressions (22) and (23).

[36] Relative sampling errors for comparisons over the two arrays illustrated in Figure 5 are shown as smooth curves in Figure 6 as a function of the gauge averaging time T, calculated using the GATE model parameters. The optimal gauge averaging time for the larger area grid box containing 49 gauges is predicted to be about 1 h, and relative error for the comparison is 30%, much lower than for the single-gauge comparisons shown in Figure 4, as expected. The same averaging time, 1 h, is best for the 1° × 1° box, though with much larger comparison errors.

[37] When the same calculations are done with TOGA COARE model parameters (not shown), the comparison errors for regularly spaced gauge arrays are predicted to be larger than 100%, and the optimal averaging time increases to several hours. It should be noted, of course, that the model used in these calculations has been fitted to oceanic radar data, whereas continental rain-rate variability, especially during the summer, is likely to be much stronger and to exhibit strong diurnal modulations.

[38] As an example of how the gauge spacing in an array affects the optimal averaging time, we show in Figure 7 the relative sampling error for a very dense 21-gauge array with gauges spaced 2 km apart and covering a circular 100-km^2 area, similar in size to a microwave instrument FOV. Note that the best averaging time is of the order of minutes rather than hours (cf. Figure 6) for this spacing, and that the sampling error estimates using the TOGA COARE parameters are considerably higher than for the GATE parameters. Minimum sampling errors range from about 60% for GATE to 250% for TOGA Cruise 1; reducing the sampling error in

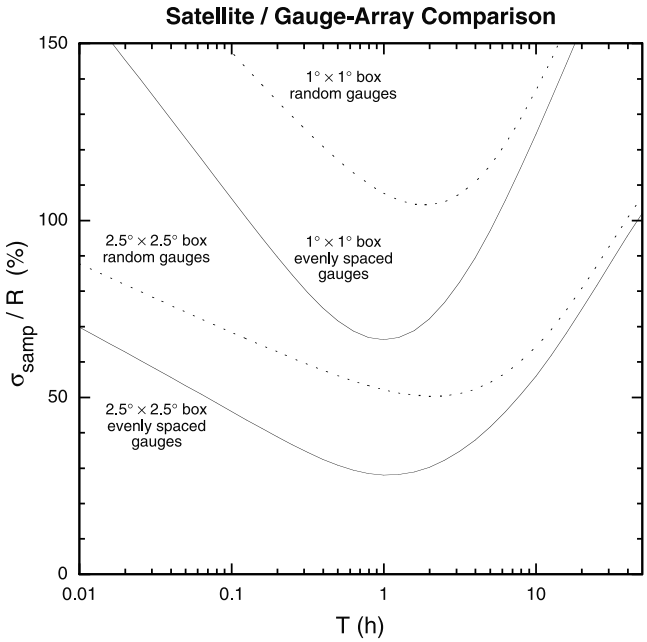

Figure 6. Model predictions of relative sampling error for comparison of a single satellite overflight over circular areas equivalent to 1° × 1° and 2.5° × 2.5° boxes containing 9 and 49 gauges respectively. Errors are plotted as a function of the time interval T over which the gauge data are averaged. Smooth curves show sampling error for gauges as depicted in Figure 5, spaced 39 km apart (similar in density to that of the Oklahoma Mesonet). Dotted curves show sampling error averaged over all possible random placements of the gauges within the areas. GATE model parameters in Table 1 were used in the calculations.

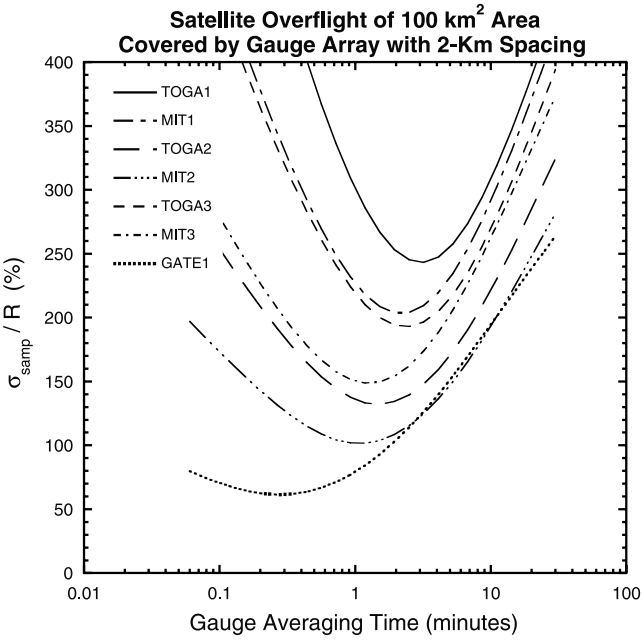

Figure 7. Model predictions of relative sampling error for comparison of a single satellite overflight over a circular 100-km^2 area containing 21 gauges spaced 2 km apart. Relative error is plotted as a function of the gauge-averaging time interval T bracketing the satellite overflight time. Parameter values in Table 1 were used in the calculations. Note change in timescale from Figure 6.

satellite/gauge comparisons to the 10% level would require averaging over anywhere from 36 to 625 satellite overflights of the array, according to these results.

4.3. Single Satellite Overflight, Random Gauges

[39] It is interesting to investigate how sensitive the results are to the idealized spacing used in the previous example. It is quite easy to calculate the average of $\sigma^2_{ng,\mathrm{samp}}$ over all possible configurations of the n gauges within the area A allowing each of the positions $\mathbf{x}_i$ to be arbitrarily assigned within A. Averaging over every possible configuration is equivalent to acting on expressions (22) and (23) with the averaging operation $(1/A)\int_A d^2\mathbf{x}_i$ for each gauge i. Except for the terms involving $[R'_T(\mathbf{x}_i)]^2$, this is equivalent to replacing $R_T(\mathbf{x}_i)$ for each gauge by R_{AT}, the space-time average of rain rates everywhere within A over the interval T, as defined in equation (A3) in Appendix A. For $c_{ng,ng}$ one obtains

$$\langle c_{ng,ng}\rangle_{\mathbf{x}} = \sigma^2_{AT} + \frac{\sigma^2_T - \sigma^2_{AT}}{n}, \tag{25}$$

with the bracket operation on the left hand side indicating an average over gauge locations, and with σ^2_T and σ^2_{AT} defined in Appendix A by equations (A13) and (A17).

[40] The remaining term in (24), averaged over gauge positions, is

$$\langle c_{s,ng}\rangle_{\mathbf{x}} = \langle R'_A R'_{AT}\rangle, \tag{26}$$

which is computed for the model in Appendix A, with the result given in equation (A25). Relative sampling error for the two cases studied in the previous subsection for randomly placed gauges is shown in Figure 6 as dotted curves. As expected, when the gauge locations become more random, comparison error tends to increase, and, perhaps less obviously, the optimal averaging time increases as well, probably because of the tendency for there to be larger gaps between the randomly placed gauges.

4.4. [Aside:] A Classic Hydrological Problem

[41] Rain-gauge arrays have long been used to estimate the average rain rate R_{AT} for a time period T over an area A covered by the array. (The total rain accumulation is given by TR_{AT}.) It is interesting to note that the mean squared error in the classic hydrological problem of determining R_{AT} with a gauge array [e.g., *Zawadzki*, 1973] is easily obtained for the random-gauge case just discussed, using (25) and $\langle R'_{ng} R'_{AT}\rangle_{\mathbf{x}} = \sigma^2_{AT}$, as

$$\sqrt{\left\langle \left(R_{ng} - R_{AT}\right)^2 \right\rangle_{\mathbf{x}}} = \sqrt{\frac{\sigma^2_T - \sigma^2_{AT}}{n}}, \tag{27}$$

which gives the approximate $n^{-1/2}$-dependence on gauge number found by *Rudolf et al.* [1994] in their studies, and indicates that the coefficient of $\sigma_T/\sqrt{n}$ they obtained is predicted to be

$$\sqrt{\left\langle \left(R_{ng} - R_{AT}\right)^2 \right\rangle_{\mathbf{x}}} = \left(\frac{\sigma^2_T - \sigma^2_{AT}}{\sigma^2_T}\right)^{1/2} \frac{\sigma_T}{\sqrt{n}}; \tag{28}$$

the coefficient $(\sigma^2_T - \sigma^2_{AT})^{1/2}/\sigma_T$ depends solely on the spatial correlation of the gauge data at averaging time T. Physically plausible spatial correlations will always produce coefficients between 0 and 1. Note that equation (28) is a consequence of equation (25) alone and does not depend on the particular model we are using. When the coefficient is calculated using the model for a case analogous to the ones studied by *Rudolf et al.* [1994], assuming a disk with area equal to that of a 2.5° × 2.5° grid box for monthly averaged gauge data, the model with GATE parameters predicts a coefficient value of 0.76, while with TOGA COARE parameters the model predicts coefficients ranging from 0.88 to 0.93, depending on the case.

[42] *Rudolf et al.* [1994] fitted their collective results for relative mean absolute error for gauge arrays in Australia, Germany, and the United States, to an approximate form $0.865 \times \sigma_T/n^{0.555}$ (neglecting a small additive constant term). Since equation (28) is written for rms error instead of mean absolute error, the coefficient 0.865 found by *Rudolf et al.* [1994] should be multiplied by $\sqrt{\pi/2}$ to be compared with the coefficient in (28), as pointed out by *McCollum and Krajewski* [1998] (who also provide an argument for the $n^{-1/2}$ dependence on gauge number seen by *Rudolf et al.* [1994]). Since $\sqrt{\pi/2} \times 0.865 = 1.1$ is greater than 1, the effects of spatial correlation of the gauges predicted by (28) do not seem to have shown up in the results obtained by *Rudolf et al.* [1994]. This may indicate the presence of greater than expected sampling error in the coefficient obtained by *Rudolf et al.* [1994], possibly due to nonnormality in the distribution of the errors, or the influence of inhomogeneity in the statistics. *Rudolf et al.* [1994] found that sampling error appeared to decrease slightly faster with gauge number than $n^{-1/2}$. This

may be due to the fact that the real gauge arrays studied by *Rudolf et al.* [1994] were not randomly distributed, since gauges in real arrays tend to be spaced a certain minimum distance apart, whereas the $n^{-1/2}$ behavior derived above depended on the assumption of complete randomness of gauge positions.

4.5. Monthly Averages, Many Satellite Visits

[43] It is clear from the above results that using rain gauge data to validate satellite estimates at the 10% level requires averaging over more than one satellite overflight of the gauges. We turn next to comparisons of monthly averaged gauge data with averages of satellite data taken in the vicinity of the gauges during the month. In this case the time interval $T = 1$ month is specified beforehand, and we investigate how σ_{samp}/R changes with A, the area around the gauge(s) over which the satellite data are averaged.

[44] The low Earth-orbiting satellites carrying microwave instruments tend to revisit a location about once per day, at least in lower latitudes, averaging about 30 visits per month. To simplify our calculations, we assume that a satellite visits a site at regular intervals Δt, and that the visit times are given by

$$t_j = t_0 + (j-1)\Delta t, \quad j = 1, \ldots, m. \tag{29}$$

The satellite average to which the gauge average R_{g} is compared is given by

$$R_{\text{s}} = \frac{1}{m}\sum_{j=1}^{m} R_A(t_j), \tag{30}$$

where $R_A(t)$ is defined in (4). Mean squared sampling error is thus given by (12), taking into account the effect of multiple satellite visits. In particular,

$$\begin{aligned} c_{\text{ss}} &= \left\langle \left(R'_{\text{s}}\right)^2 \right\rangle \\ &= \frac{1}{m^2}\sum_i \sum_j \left\langle R'_A(t_i) R'_A(t_j) \right\rangle. \end{aligned} \tag{31}$$

This can be simplified using the lagged covariance of area-averaged rain rate $c_{AA}(\tau)$, defined in Appendix A in (A31), and the identity

$$\sum_{i=1}^{m}\sum_{j=1}^{m} f(j-i) = \sum_{u=-m}^{m} (m - |u|) f(u) \tag{32}$$

to obtain

$$c_{\text{ss}} = \frac{1}{m}\sigma_A^2 + \frac{2}{m}\sum_{u=1}^{m-1}\left(1 - \frac{u}{m}\right) c_{AA}(u\Delta t), \tag{33}$$

with $\sigma_A^2 = c_{AA}(\tau = 0)$. Because $c_{AA}(\tau)$ falls off rapidly for $\tau \gg 1$ day, equation (33) is well approximated by

$$c_{\text{ss}} \approx \frac{1}{m}\left[\sigma_A^2 + 2\sum_{u=1}^{\infty} c_{AA}(u\Delta t)\right]. \tag{34}$$

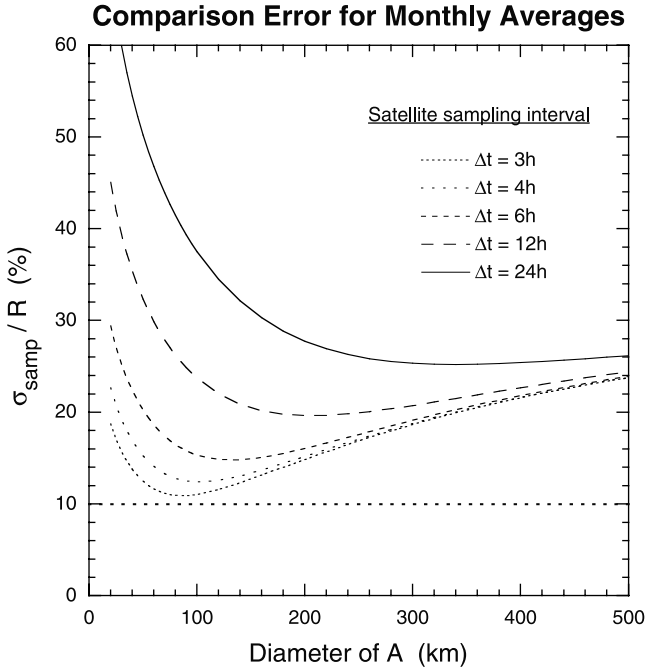

Figure 8. Relative sampling error predicted by model using GATE statistics for comparison of monthly averages of data from a single gauge with averages of all satellite estimates during the month for an area A around the gauge. The satellite is assumed to visit at intervals Δt. Satellites with microwave instruments typically visit at intervals $\Delta t \approx$ 24 h. A dashed line indicates error at the 10% level.

The cross term c_{sg} for this case,

$$c_{\text{sg}} = \frac{1}{m}\sum_{j=1}^{m} \left\langle R'_A(t_j) R'_T \right\rangle, \tag{35}$$

can likewise be well approximated by

$$c_{\text{sg}} \approx \left\langle R'_A(0) R'_T \right\rangle, \tag{36}$$

which is dealt with in equation (A19) of Appendix A. Sampling error for multiple satellite visits during $T = 1$ month can therefore be calculated from

$$\sigma_{\text{samp}}^2 \approx \sigma_T^2 + \frac{1}{m}\left[\sigma_A^2 + 2\sum_{u=1}^{\infty} c_{AA}(u\Delta t)\right] - 2c_{AT}(\mathbf{b} = 0). \tag{37}$$

Model predictions for each of the terms in (37) are obtained in Appendix A.

[45] Figure 8 shows the relative sampling error for a typical sampling interval of $\Delta t = 1$ day, and also for more frequent visits, down to the interval $\Delta t = 3$ h being discussed as a goal for an international satellite program called the Global Precipitation Measurement (GPM) mission. The optimal area for satellite averages being compared with a single rain gauge over one month is quite large, of the order of a 2.5° box for typical sampling intervals of once per day. As the satellite visit interval becomes shorter, the optimal area for averaging shrinks, to one smaller than a 1° box for a GPM-like case. Note that a month of averaging is still not sufficient for achieving comparisons at the 10%

level. If we assume that relative sampling error using M months of data will decrease by a factor $M^{-1/2}$ from the sampling error for 1 month, approximately 6 months would be required to reach the 10% level for validation of a single satellite's estimates—or more gauges within the area are required. With two gauges, for instance, the required averaging time (not shown) drops to about 4 months. In a GPM-like era with the equivalent of 3-hourly satellite visits to a gauge site it may be possible to establish bias levels at the 10% level in a single month with just a few gauges in an area. It should be noted that the above estimates are based on GATE parameters, which tend to give smaller sampling-error estimates than may generally be the case.

5. Time-Weighted Gauge Data

[46] The comparison of long time averages of gauge data with averages of satellite data in the previous section used straightforward averaging of the gauge data. Suppose one were to allow the weighting of the gauge data to vary in time depending on how far away in time the gauge observation is from a satellite overflight occurrence? In this section we look at a simplified version of this proposition to obtain an estimate of how much improvement in the validation procedure might be possible by using time-weighted averages of the gauge data.

[47] As an example, assume that the gauge data are available at hourly intervals for a period H hours in length, of the order of a month or more. The gauge data are therefore provided as a sequence of hourly averages $R_T(t_j)$, $T = 1$ h, $j = 1, \ldots, H$, where $R_T(t)$ is the time-averaged gauge data over an interval T centered on time t, as defined in Appendix A in (A26). The time-weighted gauge average is

$$R_{g,w} = \frac{1}{H}\sum_{j=1}^{H} w_j R_T(t_j). \tag{38}$$

The weighting must preserve the long-term mean rain rate, so we require the weights w_j to satisfy

$$\sum_{j=1}^{H} w_j = H. \tag{39}$$

We expect the weights to emphasize gauge data taken near the satellite observation times and de-emphasize data taken far from the satellite observation times.

[48] To simplify the problem, assume that the interval between satellite visits, Δt, is an integral number of hours, and that N satellite overflights occur during the averaging period H. The satellite average rain rate is

$$R_s = \frac{1}{N}\sum_{q=1}^{N} R_A(t_q), \tag{40}$$

where the satellite visit times are given by t_q, $q = 1, \ldots, N$, at intervals $t_{q+1} - t_q = \Delta t$. The weights w_j must then be found that minimize the variance of the scatter of R_s about $R_{g,w}$,

$$\sigma^2_{\text{samp},w} = \left\langle \left(R_s - R_{g,w}\right)^2 \right\rangle. \tag{41}$$

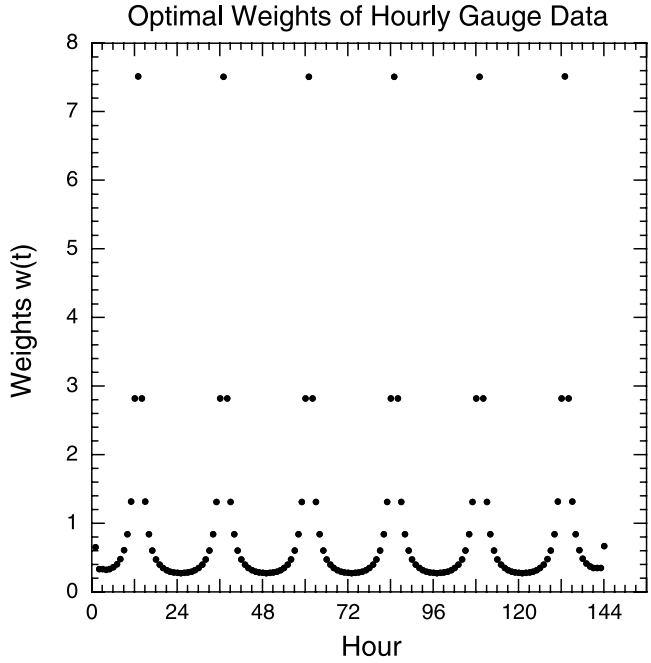

Figure 9. Optimal weights of hourly gauge data for comparison with averages of satellite data provided every 24 h over a 126-km diameter area centered on the gauge, assuming GATE statistics, for 6 days of satellite data.

This is a standard minimization problem, requiring minimization of (41) with the constraint (39) included by adding it to $\sigma^2_{\text{samp},w}$ as a Lagrange multiplier term:

$$\mathcal{L} = \left\langle \left(R_s - R_{g,w}\right)^2 \right\rangle - \frac{2\lambda}{H}\sum_{j=1}^{H} w_j. \tag{42}$$

The factor $(-2/H)$ has been included with the Lagrange multiplier λ for convenience.

[49] The optimal weights w_j are determined by the equations $\partial\mathcal{L}/\partial w_j = 0$, $j = 1, \ldots, H$, or

$$\frac{1}{H}\sum_{j'=1}^{H} c_{gg}(t_{j'} - t_j) w_{j'} - \frac{1}{N}\sum_{q=1}^{N} c_{sg}(t_q - t_j) - \lambda = 0, \tag{43}$$

with λ determined by the constraint equation (39), where the lagged gauge covariance terms $c_{gg}(t_{j'} - t_j)$ are provided in Appendix A by equation (A28), and the lagged satellite-gauge covariance terms $c_{sg}(t_q - t_j)$ are provided by equation (A30). Equations (43) are linear in the weights w_j and can be solved using standard methods. Once the w_j are known, the value of $\sigma^2_{\text{samp},w}$ can be computed from (41), using (33) for $\langle (R'_s)^2 \rangle$. Appendix B gives some additional information about solving (43) for the weights and obtaining the sampling error $\sigma^2_{\text{samp},w}$.

[50] Figure 9 shows the optimal weights obtained using GATE parameters for comparison of an area equivalent to a $1^\circ \times 1^\circ$ box with a single gauge at the center providing 1-h average rain rates, assuming that the satellite returns every 24 h. The calculation is done for a 6-day period, and shows that once the "end effects" have subsided the weights settle into a regular repeating pattern for the interior hours. The

optimal weights indicate, as expected, that it is the hour of gauge data bracketing the satellite visit that should be weighted most, contributing about 30% to the weighted average (7.5/24). The sampling error variance $\sigma^2_{\text{samp},w}$ for the optimal weighting is reduced to about 50% of the error variance for uniform weighting σ^2_{samp}.

[51] The amount of reduction in sampling error provided by adding time-varying weighting depends on the area A and the parameter values of the model, among other factors. For instance, if the parameters in Table 1 for TOGA Cruise 1 are used, the error variance is only reduced to about 80% of the variance for uniform weighting. The reduction in variance is larger, percentage-wise, for smaller areas, but the error variance also gets worse as the area shrinks, as shown in Figure 4. It is not clear that generalizations about the best approach for satellite/gauge comparisons can be made, since it depends so much on the characteristics of the data in each case.

6. Discussion and Conclusions

[52] Rain gauges provide such direct measurements of rainfall that testing remote sensing estimates of rainfall against gauge observations is extremely attractive. The high spatial and temporal variability of rain, however, makes comparisons of the two difficult. One of the choices that must be made in such comparisons is how much averaging of the gauge data and satellite data are needed in order to reduce the "noisiness" of the comparisons to a level low enough that they can be informative. A spectral model was used to examine some of these questions because it captures one of the more subtle statistical features of rain: the linking of characteristic times for changes in areal averages to the size of the averaging area.

[53] Although the model parameters were adjusted to fit the statistics of radar-derived rain rates (rather than of gauge data) over two tropical oceanic regions, the model seems to capture many of the statistical characteristics of gauge data as well. The model parameters obtained from the fits to radar data may cause the model to underestimate the amount of small-scale variability on timescales of a fraction of an hour and the amount of large-scale variability on timescales of a week or more. Based on some limited experiments, it is likely that increased small-scale variability will make intercomparisons noisier, whereas increased large-scale variability will probably make intercomparisons more informative.

[54] As Table 1 makes clear, the parameters in the spectral model change depending on the data set used to estimate them. The calculations described here provide some examples of how large sampling error in satellite/gauge comparisons might be, but even over the oceanic areas from which the Table 1 data were gathered the model predictions are likely to represent the true rms errors for comparisons at only a factor-of-2 level of accuracy. The results should, however, be able to serve as a guide for how sampling errors in satellite/gauge comparisons might depend on the comparison areas, periods, and gauge densities.

[55] The spectral model assumes that the statistics of rain (not rain rates themselves, of course) are the same everywhere in the comparison area and at all times during the averaging periods. The model covariance of rain rate at two points separated in space and/or time depends only on their separation (as in equation (11)), not on their absolute locations. It is possible to develop models that describe covariance statistics that depend on location or, for instance, the time of day. Empirical orthogonal functions (EOFs) can be used to describe inhomogeneous covariance statistics. *Shen et al.* [1994], for example, use them to obtain optimal weights for estimating global average temperature from isolated station data around the world. *Kim and North* [1997] propose a type of EOF that can in principle describe statistics that change with the time of day. When compared with temperature, however, rain rates at gauge scales are so highly variable that it may require many decades of data over a dense gauge network to obtain stable estimates of the EOFs needed for such approaches.

[56] The model indicates that comparisons of rain estimates from single satellite-instrument footprints in the neighborhood of a single gauge are too noisy to be of much use—a fact well documented in many examinations of such comparisons. If areal averaging of the satellite data is used to reduce sampling noise, the model indicates that there is an optimal averaging time for the gauge data for best comparisons, and that the optimal time increases with the area. Comparisons of data from a single gauge and a single satellite overflight, however, require averaging times and areas that are too large to be practical.

[57] The situation is improved when multiple gauges are present in the area observed by the satellite during its overflight. Even gauge densities as high as 1 per 1000 km^2 in a 2.5° × 2.5° box, however, are unlikely to bring comparison errors down to the 10% level. Averaging over multiple overflights of the gauges is required. For a typical passive-microwave-instrument-bearing satellite providing about 30 visits per month, the optimal averaging area around a single gauge is about that of a 2.5° × 2.5° box, and time averaging over a substantial part of a year is required to bring sampling errors down to the 10% level. The optimal averaging area and time decreases when more gauges are present. Multiple satellites with similar instruments providing more than 1 visit per day can also decrease the averaging time required. For satellite visits every 3 h, for example, a single month of averaging might suffice.

[58] Finally, the improvements in satellite/gauge comparisons that might be possible if the gauge data are weighted depending on their relationship in time to the satellite overflight times indicates that substantial reduction in the scatter of the gauge and satellite averages is possible using this technique, though the amount of improvement varies considerably with the situation.

Appendix A: Details of Model Calculations

[59] Many of the results presented in this paper require calculations of variances and covariances of spatial and temporal averages of the rain-rate field based on the point covariance function in equation (11) and the spectral model in equations (16)–(18). By carrying out the spatial averages over circular areas A ($A = \pi a^2$) instead of the more traditional square areas, calculations are made much simpler. A number of results useful in carrying out the calculations in a numerically efficient manner are collected in this appendix. Both the algebraic and numerical results presented in this

paper were obtained with the help of Mathematica software (version 4 [see *Wolfram*, 1999]).

[60] To simplify notation, define the instantaneous area-averaged rain rate (identical to equation (4)) at time t as

$$R_A(t) = \frac{1}{A}\int_A d^2\mathbf{x}\, R(\mathbf{x}, t), \tag{A1}$$

the time-averaged rain rate for a gauge located at a point $\mathbf{b}$ relative to the center of the area A as

$$R_T(\mathbf{b}) = \frac{1}{T}\int_{-T/2}^{T/2} dt\, R(\mathbf{b}, t), \tag{A2}$$

and the area-time averaged rain rate as

$$R_{AT} = \frac{1}{AT}\int_A d^2\mathbf{x}\int_{-T/2}^{T/2} dt\, R(\mathbf{x}, t). \tag{A3}$$

[61] We give as an example some of the steps needed in obtaining a simple integral expression for the variance of R_A,

$$\sigma_A^2 \equiv \left\langle \left(R'_A\right)^2 \right\rangle = \left\langle \frac{1}{A^2}\int_A d^2\mathbf{x}\int_A d^2\mathbf{y}\, R'(\mathbf{x}, 0)R'(\mathbf{y}, 0)\right\rangle \tag{A4}$$

$$= \frac{1}{A^2}\int_A d^2\mathbf{x}\int_A d^2\mathbf{y}\, c(\mathbf{x}-\mathbf{y}, 0) \tag{A5}$$

using equation (11). Substituting equation (16) we obtain

$$\sigma_A^2 = \frac{1}{A^2}\int_A d^2\mathbf{x}\int_A d^2\mathbf{y}(2\pi)^{-3/2} \cdot \int d^2\mathbf{k}\int d\omega\, e^{i\mathbf{k}\cdot(\mathbf{x}-\mathbf{y})}\tilde{c}(\mathbf{k}, \omega). \tag{A6}$$

Since $\tilde{c}$ ($\mathbf{k}$, ω) does not depend on the direction of $\mathbf{k}$, the areal integrals can be done using

$$\int_A d^2\mathbf{x}\, e^{i\mathbf{k}\cdot\mathbf{x}} = \int_0^a r dr\int_0^{2\pi} d\phi\, e^{ikr\cos\phi} = 2\pi a^2 J_1(ka)/(ka), \tag{A7}$$

where $J_m(x)$ is the Bessel function of the first kind [see, e.g., *Dwight*, 1961], and the integral over ω in (A6) with $\tilde{c}(\mathbf{k}, \omega)$ in (17) gives

$$\int_{-\infty}^{\infty} d\omega\, \tilde{c}(k, \omega) = \pi F_0 \tau_k. \tag{A8}$$

After some algebra, one obtains from (A6)

$$\sigma_A^2 = \frac{4\gamma'_0}{\alpha^2}\int_0^\infty \frac{d\kappa}{\kappa}\frac{J_1^2(\kappa)}{\nu(\kappa/\alpha)} \tag{A9}$$

with the definitions

$$\gamma'_0 = \Gamma(1+\nu)\gamma_0, \tag{A10}$$

$$\alpha = a/L_0, \tag{A11}$$

and

$$\nu(z) = \left(1+z^2\right)^{1+\nu}. \tag{A12}$$

[62] The variance of $R_T(\mathbf{b})$ defined in (A2), which does not depend on position $\mathbf{b}$, can be calculated with an approach similar to the one above, yielding

$$\sigma_T^2 \equiv \left\langle R_T'^2 \right\rangle \tag{A13}$$

$$= \frac{2\gamma'_0}{u}\int_0^\infty d\kappa\, \frac{\kappa}{\nu^2(\kappa)} h(\kappa; u), \tag{A14}$$

with

$$u \equiv T/\tau_0 \tag{A15}$$

and

$$h(\kappa; u) \equiv 1 - \frac{1}{u\nu(\kappa)}\left[1 - e^{-u\nu(\kappa)}\right]. \tag{A16}$$

Likewise, the variance of R_{AT} defined in (A3) can be calculated to be

$$\sigma_{AT}^2 \equiv \left\langle R_{AT}'^2 \right\rangle \tag{A17}$$

$$= \frac{8\gamma'_0}{u\alpha^2}\int_0^\infty \frac{d\kappa}{\kappa}\frac{J_1^2(\kappa)}{\nu^2(\kappa/\alpha)} h(\kappa/\alpha; u). \tag{A18}$$

[63] A number of covariances are also needed, and these are calculated in a manner similar to the example given above. The covariance of $R_A(t = 0)$ with a gauge average $R_T(\mathbf{b})$ is given by

$$c_{AT}(b) \equiv \left\langle R'_A R'_T(\mathbf{b})\right\rangle \tag{A19}$$

$$= \frac{4\gamma'_0}{u\alpha^2}\int_0^\infty d\kappa\, \frac{J_1(\kappa)J_0(\beta\kappa/\alpha)}{\nu^2(\kappa/\alpha)}\left[1 - e^{-(u/2)\nu(\kappa/\alpha)}\right] \tag{A20}$$

with

$$\beta \equiv b/L_0. \tag{A21}$$

The covariance of time averages of gauge data for two gauges separated by a distance $\mathbf{b}$ is given by

$$c_{TT}(b) \equiv \left\langle R'_T(\mathbf{b})R'_T(0)\right\rangle \tag{A22}$$

$$= \frac{2\gamma'_0}{u}\int_0^\infty d\kappa \frac{\kappa J_0(\beta\kappa)}{\nu^2(\kappa)} h(\kappa; u). \tag{A23}$$

The spatial correlation of the gauges is, of course, given by $c_{TT}(b)/c_{TT}(0)$.

[64] The covariance of spatial averages with space-time averages needed for equation (26) is given by

$$c_{A,AT} \equiv \left\langle R'_A R'_{AT}\right\rangle \tag{A24}$$

$$= \frac{8\gamma'_0}{u\alpha^2}\int_0^\infty \frac{d\kappa}{\kappa}\frac{J_1^2(\kappa)}{\nu^2(\kappa/\alpha)}\left[1 - e^{-(u/2)\nu(\kappa/\alpha)}\right]. \tag{A25}$$

[65] The calculation of optimal time-dependent weighting of gauge data for comparison with satellite estimates requires formulas for the lagged covariance of gauge averages and satellite areal averages. First, define the gauge average centered around time t_0 as

$$R_T(t_0) \equiv \frac{1}{T}\int_{-T/2}^{T/2} dt\, R(0, t_0 + t). \tag{A26}$$

The covariance of two gauge averages with averaging interval T lagged by time τ is given by

$$c_{TT}(\tau; T) \equiv \left\langle R'_T(\tau) R'_T(0) \right\rangle \tag{A27}$$

$$= \frac{2\gamma'_0}{u^2}\int_0^\infty d\kappa\, \kappa \frac{e^{-|\tau/\tau_0|\nu(\kappa)}}{\nu^3(\kappa)}\ \sinh^2[u\nu(\kappa)/2], \tag{A28}$$

valid for $|\tau| \geq T$. The lagged covariance of an instantaneous average over a circular area A at $t = 0$ with a gauge average lagged by τ is given by

$$c_{AT}(\tau; T) \equiv \left\langle R'_A(0) R'_T(\tau) \right\rangle \tag{A29}$$

$$= \frac{4\gamma'_0}{u\alpha^2}\int_0^\infty d\kappa\, \frac{J_1(\kappa) e^{-|\tau/\tau_0|\nu(\kappa/\alpha)}}{\nu^2(\kappa/\alpha)} \sinh[u\nu(\kappa/\alpha)/2], \tag{A30}$$

valid for $|\tau| \geq T/2$. Finally, the covariance of instantaneous area-averaged rain rate separated by a time interval τ is given by

$$c_{AA}(\tau) \equiv \left\langle R'_A(\tau) R'_A(0) \right\rangle \tag{A31}$$

$$= \frac{4\gamma'_0}{\alpha^2}\int_0^\infty \frac{d\kappa}{\kappa}\, \frac{J_1^2(\kappa)}{\nu(\kappa/\alpha)}\ e^{-|\tau/\tau_0|\nu(\kappa/\alpha)}. \tag{A32}$$

Using this result, the bracketed sum in equation (37) can be carried out inside the integral in (A32) using $\Sigma_{j=0}^{\infty} z^j = 1/(1 - z)$ to yield

$$\sigma_A^2 + 2\sum_{u=1}^{\infty} c_{AA}(u\Delta t) = \frac{4\gamma'_0}{\alpha^2} \cdot \int_0^\infty \frac{d\kappa}{\kappa}\, \frac{J_1^2(\kappa)}{\nu(\kappa/\alpha)} \coth[-|\Delta t/\tau_0|\, \nu(\kappa/\alpha)/2]. \tag{A33}$$

Appendix B: Optimal Weight Solution

[66] In section 5 of the paper equations (43) for the optimal weights of gauge data are obtained. They are fairly simple to solve for the weights using standard linear-algebra methods. We present here a brief description of the approach we have used.

[67] Rewrite equations (43) in a form amenable to methods for solving sets of simultaneous linear equations by defining the weight vector $\mathbf{w}$,

$$(\mathbf{w})_j = w_j, \tag{B1}$$

the symmetric covariance matrix,

$$(\mathsf{C})_{jj'} = c_{\mathrm{gg}}(t_{j'} - t_j), \tag{B2}$$

and the vector defined by the middle term of (43), summed over all satellite overflight times, as

$$(\mathbf{d})_j = \frac{1}{N}\sum_{q=1}^{N} c_{\mathrm{sg}}(t_q - t_j). \tag{B3}$$

It is also convenient to introduce a vector consisting entirely of 1's,

$$(\mathbf{1})_j = 1, \quad j = 1, \ldots, H. \tag{B4}$$

Using the above definitions, equation (43) can be written in vector notation as

$$H^{-1}\,\mathsf{C}\mathbf{w} - \mathbf{d} - \lambda\mathbf{1} = 0, \tag{B5}$$

with the constraint equation (39) for $\mathbf{w}$ written as

$$\mathbf{1}^{\mathsf{T}}\mathbf{w} = H, \tag{B6}$$

where the superscript T indicates matrix transpose (e.g., $\mathbf{w} \cdot \mathbf{d} = \mathbf{w}^{\mathsf{T}}\mathbf{d}$). Equation (B5) is readily solved for the weights as

$$\mathbf{w} = H\mathsf{C}^{-1}(\mathbf{d} + \lambda\mathbf{1}), \tag{B7}$$

where λ is determined by the constraint equation (B6) and solution (B7) to be

$$\lambda = \frac{1 - \mathbf{1}^{\mathsf{T}}\mathsf{C}^{-1}\mathbf{d}}{\mathbf{1}^{\mathsf{T}}\mathsf{C}^{-1}\mathbf{1}}. \tag{B8}$$

The solution requires obtaining the inverse matrix $\mathbf{C}^{-1-1}$, which is a standard numerical problem.

[68] Once the weights are obtained, the sampling error for the difference of the satellite average from the time-weighted gauge average can be obtained from (41) as

$$\begin{aligned}\sigma^2_{\mathrm{samp},w} &= \left\langle \left(R'_{\mathrm{s}}\right)^2 \right\rangle + \left\langle \left(R'_{\mathrm{g},w}\right)^2 \right\rangle - 2\left\langle R'_{\mathrm{s}} R'_{\mathrm{g},w} \right\rangle \\ &= \left\langle \left(R'_{\mathrm{s}}\right)^2 \right\rangle + H^{-2}\mathbf{w}^{\mathsf{T}}\mathsf{C}\mathbf{w} - 2H^{-1}\mathbf{w}^{\mathsf{T}}\mathbf{d} \\ &= c_{\mathrm{ss}} + H^{-1}\mathbf{w}^{\mathsf{T}}(\mathbf{d} + \lambda\mathbf{1}) - 2H^{-1}\mathbf{w}^{\mathsf{T}}\mathbf{d} \\ &= c_{\mathrm{ss}} + \lambda - H^{-1}\mathbf{w}^{\mathsf{T}}\mathbf{d}\end{aligned} \tag{B9}$$

using equations (38), (B2), and (B3) for the first step above, equation (B5) for the second step, and the constraint equation (B6) for the last step. Equation (33) provides an exact expression for c_{ss}.

[69] **Acknowledgments.** We wish to thank Witold F. Krajewski and the reviewers of the manuscript, Gerald R. North, Samuel S. P. Shen, and Matthias Steiner, for many excellent suggestions for improving the paper, and Tom Keenan for helpful comments. This research was supported by the Office of Earth Science of the National Aeronautics and Space Administration as part of the Tropical Rainfall Measuring Mission.

References

Abtew, W., J. Obeysekera, and G. Shih, Spatial variation of daily rainfall and network design, *Trans. Am. Soc. Agric. Eng.*, *38*, 843–845, 1995.

Bell, T. L., A space-time stochastic model of rainfall for satellite remote-sensing studies, *J. Geophys. Res.*, *92*, 9631–9643, 1987.

Bell, T. L., and P. K. Kundu, A study of the sampling error in satellite rainfall estimates using optimal averaging of data and a stochastic model, *J. Clim.*, *9*, 1251–1268, 1996.

Berg, W., and S. K. Avery, Evaluation of monthly rainfall estimates derived from the special sensor microwave/imager (SSM/I) over the tropical Pacific, *J. Geophys. Res.*, *100*, 1295–1315, 1995.

Brock, F. V., K. C. Crawford, R. L. Elliott, G. W. Cuperus, S. J. Stadler, H. L. Johnson, and M. D. Eilts, The Oklahoma Mesonet: A technical overview, *J. Atmos. Oceanic Technol.*, *12*, 5–19, 1995.

Ciach, G. J., W. F. Krajewski, E. N. Anagnostou, M. L. Baeck, J. A. Smith, J. R. McCollum, and A. Kruger, Radar rainfall estimation for ground validation studies of the Tropical Rainfall Measuring Mission, *J. Appl. Meteorol.*, *36*, 735–747, 1997.

Court, A., Reliability of hourly precipitation data, *J. Geophys. Res.*, *65*, 4017–4024, 1960.

Dwight, H. B., *Tables of Integrals and Other Mathematical Data*, Macmillan, Old Tappan, N. J., 1961.

Ebert, E. E., M. J. Manton, P. A. Arkin, R. J. Allam, G. E. Holpin, and A. Gruber, Results from the GPCP algorithm intercomparison programme, *Bull. Am. Meteorol. Soc.*, *77*, 2875–2887, 1996.

Fuller, W. A., *Measurement Error Models*, John Wiley, New York, 1987.

Graves, C. E., J. B. Valdés, S. S. P. Shen, and G. R. North, Evaluation of samplng errors of precipitation from spaceborne and ground sensors, *J. Appl. Meteorol.*, *32*, 374–385, 1993.

Ha, E., and G. R. North, Error analysis for some ground validation designs for satellite observations of precipitation, *J. Atmos. Oceanic Technol.*, *16*, 1949–1957, 1999.

Ha, E., G. R. North, C. Yoo, and K.-J. Ha, Evaluation of some ground truth designs for satellite estimates of rain rate, *J. Atmos. Oceanic Technol.*, *19*, 65–73, 2002.

Habib, E., W. F. Krajewski, V. Nešpor, and A. Kruger, Numerical simulation studies of raingage data correction due to wind effect, *J. Geophys. Res.*, *104*, 19,723–19,734, 1999.

Habib, E., W. F. Krajewski, and G. J. Ciach, Estimation of rainfall interstation correlation, *J. Hydrometeorol.*, *2*, 621–629, 2001.

Houze, R. A., Jr., and A. K. Betts, Convection in GATE, *Rev. Geophys.*, *19*, 541–576, 1981.

Hudlow, M. D., and V. L. Patterson, GATE radar rainfall atlas, technical report, Environ. Data and Inf. Serv., Natl. Oceanic and Atmos. Admin., Silver Spring, Md., 1979.

Kim, K.-Y., and G. R. North, EOFs of harmonizable cyclostationary processes, *J. Atmos. Sci.*, *54*, 2416–2427, 1997.

Krajewski, W. F., G. J. Ciach, J. R. McCollum, and C. Bacotiu, Initial validation of the Global Precipitation Climatology Project monthly rainfall over the United States, *J. Appl. Meteorol.*, *39*, 1071–1086, 2000.

Laughlin, C. R., On the effect of temporal sampling on the observation of mean rainfall, in *Precipitation Measurements From Space*, *Workshop Report*, edited by D. Atlas and O. W. Thiele, pp. D59–D66, NASA Goddard Space Flight Cent., Greenbelt, Md., 1981.

McCollum, J. R., and W. F. Krajewski, Uncertainty of monthly rainfall estimates from rain gauges in the Global Precipitation Climatology Project, *Water Resour. Res.*, *34*, 2647–2654, 1998.

McPhaden, M. J., et al., The tropical ocean-global atmosphere observing system: A decade of progress, *J. Geophys. Res.*, *103*, 14,169–14,240, 1998.

Mooley, D. A., and P. M. M. Ismail, Structure functions of rainfall field and their application to network design in the tropics, *Arch. Meteorol. Geophys. Bioklimatol., Ser. B*, *30*, 95–105, 1982.

Morrissey, M. L., Using sparse raingages to test satellite-based rainfall algorithms, *J. Geophys. Res.*, *96*, 18,561–18,571, 1991.

Morrissey, M. L., J. A. Maliekal, J. S. Greene, and J. Wang, The uncertainty of simple spatial averages using rain gauge networks, *Water Resour. Res.*, *31*, 2011–2017, 1995.

Nešpor, V., and B. Sevruk, Estimation of wind-induced error of rainfall gauge measurements using a numerical simulation, *J. Atmos. Oceanic Technol.*, *16*, 450–464, 1999.

North, G. R., and S. Nakamoto, Formalism for comparing rain estimation designs, *J. Atmos. Oceanic Technol.*, *6*, 985–992, 1989.

North, G. R., J. B. Valdés, E. Ha, and S. S. P. Shen, The ground-truth problem for satellite estimates of rain rate, *J. Atmos. Oceanic Technol.*, *11*, 1035–1041, 1994.

Olson, W. S., Physical retrieval of rainfall rates over the ocean by multispectral microwave radiometry: Application to tropical cyclones, *J. Geophys. Res.*, *94*, 2267–2280, 1989.

Olson, W. S., C. Kummerow, G. Heymsfield, and L. Giglio, A method for combined passive-active microwave retrievals of cloud and precipitation profiles, *J. Appl. Meteorol.*, *35*, 1763–1789, 1996.

Rodríguez-Iturbe, I., and J. M. Mejía, The design of rainfall networks in time and space, *Water Resour. Res.*, *10*, 713–728, 1974a.

Rodríguez-Iturbe, I., and J. M. Mejía, On the transformation of point rainfall to areal rainfall, *Water Resour. Res.*, *10*, 729–735, 1974b.

Rodríguez-Iturbe, I., D. R. Cox, and V. Isham, Some models for rainfall based on stochastic point processes, *Proc. R. Soc. London, Ser. A*, *410*, 269–288, 1987.

Rudolf, B., H. Hauschild, W. Rueth, and U. Schneider, Terrestrial precipitation analysis: Operational method and required density of point measurements, in *Global Precipitations and Climate Change*, *NATO ASI Ser.*, vol. 1, edited by M. Desbois and F. Desalmand, pp. 173–186, Springer-Verlag, New York, 1994.

Serra, Y. L., P. A'Hearn, H. P. Freitag, and M. J. McPhaden, ATLAS self-siphoning rain gauge error estimates, *J. Atmos. Oceanic Technol.*, *18*, 1989–2002, 2001.

Shen, S. S. P., G. R. North, and K.-Y. Kim, Spectral approach to optimal estimation of the global average temperature, *J. Clim.*, *7*, 1999–2007, 1994.

Short, D. A., P. A. Kucera, B. S. Ferrier, J. C. Gerlach, S. A. Rutledge, and O. W. Thiele, Shipboard radar rainfall patterns within the TOGA COARE IFA, *Bull. Am. Meteorol. Soc.*, *78*, 2817–2836, 1997.

Silverman, B. A., L. K. Rogers, and D. Dahl, On the sampling variance of raingage networks, *J. Appl. Meteorol.*, *20*, 1468–1478, 1981.

Smith, J. A., and W. F. Krajewski, Statistical modeling of space-time rainfall using radar and rain gage observations, *Water Resour. Res.*, *23*, 1893–1900, 1987.

Waymire, E., V. K. Gupta, and I. Rodríguez-Iturbe, A spectral theory of rainfall intensity at the meso-β scale, *Water Resour. Res.*, *20*, 1453–1465, 1984.

Webster, P. J., and R. Lukas, TOGA COARE: The Coupled Ocean-Atmosphere Response Experiment, *Bull. Am. Meteorol. Soc.*, *73*, 1377–1416, 1992.

Wilheit, T. T., Error analysis for the Tropical Rainfall Measuring Mission, in *Tropical Rainfall Measurements*, edited by J. S. Theon and N. Fugono, pp. 377–385, A. Deepak, Hampton, Va., 1988.

Wolfram, S., *The Mathematica Book*, 4th ed., Cambridge Univ. Press, New York, 1999.

Wood, S. J., D. A. Jones, and R. J. Moore, Accuracy of rainfall measurement for scales of hydrological interest, *Hydrol. Earth Syst. Sci.*, *4*, 531–543, 2000.

Yoo, C., J. B. Valdés, and G. R. North, Stochastic modeling of multidimensional precipitation fields considering spectral structure, *Water Resour. Res.*, *32*, 2175–2187, 1996.

Zawadzki, I. I., Errors and fluctuations of rain gauge estimates of areal rainfall, *J. Hydrol.*, *18*, 243–255, 1973.

T. L. Bell and P. K. Kundu, NASA Goddard Space Flight Center, Mail Code 913, Greenbelt, MD 20771, USA. (bell@climate.gsfc.nasa.gov; kundu@climate.gsfc.nasa.gov)